

## Bifurcation Cascade in a Semiconductor Laser Subject to Optical Feedback

Angela Hohl and Athanasios Gavrielides

*Nonlinear Optics Group, Air Force Research Laboratory DELO, Kirtland AFB, Albuquerque, New Mexico 87117-5776*

(Received 17 March 1998)

We investigated a single mode semiconductor laser system pumped near threshold and subject to optical feedback from a short distance. We found both experimentally and numerically that as the feedback strength is increased the laser undergoes a cascade of bifurcations as one external cavity mode becomes unstable and the next one with higher intensity becomes stable only to be destabilized and replaced by the next stable external cavity mode. In the stable regions the laser operates in the so-called maximum gain mode and the unstable regions exhibit chaos which evolves into low-frequency fluctuations characterized by intensity dropouts. [S0031-9007(98)08369-0]

PACS numbers: 42.65.Sf, 42.55.Px

Feedback-induced delay systems are pervasive in a number of fields such as physiology, neurology, and optical systems [1]. Such systems are characterized by a very complex and high-dimensional dynamical behavior. A semiconductor laser subject to delayed optical feedback is an example that has received much attention. It often exhibits perplexing dynamical behavior that is not only of interest to delay problems in general but that is also of great importance in technological applications, as it may lead to performance enhancement or degradation [2].

When a semiconductor laser subject to optical feedback is pumped near its threshold it typically operates in the low-frequency fluctuation (LFF) regime. This region is characterized by irregularly occurring intensity dropouts which were first observed by Risch and Voumard [3] using a bandwidth limited detector. Fischer *et al.* [4] performed high bandwidth streak camera experiments and discovered that the intensity exhibits irregular pulses with a duration of a few tens of picoseconds which had been predicted by Tartwijk *et al.* [5]. Tkach and Chraplyvy [6] classified the effects due to feedback for a laser pumped above threshold and found that the LFF regime occurred for moderate feedback strength, and for strong feedback the laser becomes stable which was experimentally observed by Temkin *et al.* [7]. A random switching between stable and unstable operation was observed by Besnard *et al.* [8]. Sano [9] discovered that the dropout events are initiated by a crisis, a collision of a chaotic attractor with an unstable saddle.

This Letter reports the first experimental observation of a bifurcation cascade in a semiconductor laser subject to optical feedback. We compute a numerical bifurcation diagram using the Lang-Kobayashi equations [10] and find a cascade of bifurcations in accordance with our experimental results. With increasing feedback strength we find experimentally and numerically that the laser successively operates in a series of external cavity modes (ECMs); each of them is initially stable, then becomes dynamically unstable through a Hopf bifurcation, exhibits chaos which evolves into LFFs before it is replaced by the next ECM,

which is stable at first, and then follows a similar route into instability. In the stable regimes the laser operates in the maximum gain mode [11] which is accessible to the system, contrary to the predictions in [5]. Experimentally we observed coexistences between the LFFs and the stable maximum gain mode and numerically we found that the LFF trajectory stabilizes at the maximum gain mode after sufficiently long integration, which suggests that the LFF trajectory may wander close to the chaotic saddle for a very long time before escaping to an attractor.

In the experiment we used a laser diode operating at about 780 nm (SDL 5301). The laser was pumped near threshold,  $I_{th} = 25.2$  mA, and placed into a short external cavity consisting of a holographic grating and a 99% reflecting mirror similar to the setup used in [12]. The zeroth order of the grating was used to monitor the output and the first order was reflected back into the cavity. The grating had 1200 grooves per mm and was oriented at  $45^\circ$ , narrowing the cavity bandwidth to an estimated 50 GHz which is one-third of the solitary laser mode spacing. Consequently, the laser subject to optical feedback operated in a single solitary laser mode. The external cavity was 15-cm long, resulting in an ECM spacing of 1 GHz which was clearly resolved in the scanning Fabry-Perot interferometer (Newport SR-240C, free spectral range of 2000 GHz). The feedback strength was varied by a set of two polarizers and measured as a percentage of threshold reduction,  $\Delta i = (I_{th} - I)/I_{th}$ . We detected the intensity with a slow dc-coupled detector (New Focus 1801) and we used a fast ac-coupled photodetector (Hamamatsu C4258), two amplifiers, and a digitizer (Tektronix RTD 720) to capture time series with a bandwidth of 500 MHz. We also recorded power spectra using a spectrum analyzer (HP 8596E).

Figure 1 shows the experimentally observed bifurcation cascade for a pump current of  $I = 25.0$  mA obtained by monitoring the optical spectrum. For zero feedback the system operates in many solitary laser modes, and we have plotted the trace of one mode (mode 1) located at 0 GHz in Fig. 1, but the intensity is so weak that

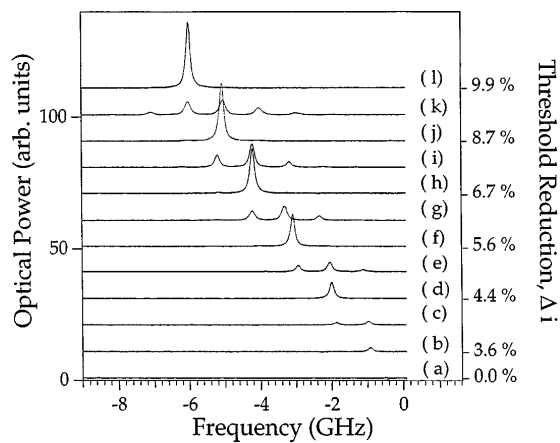


FIG. 1. Experimental bifurcation cascade in a semiconductor laser pumped near threshold and subject to optical feedback. As the feedback strength is increased, measured by the amount of threshold reduction  $\Delta i$ , the laser undergoes a cascade of bifurcations as one ECM becomes unstable and the next one with higher intensity becomes stable only to be destabilized and replaced by the next stable ECM. Traces (b), (d), (f), (h), (j), and (l) depict the laser in a stable state with a narrow line and no sidebands. Traces (c), (e), (g), (i), and (k) depict the laser in an unstable state, the laser line is broadened and has sidebands at the relaxation oscillation frequency.

the small peak is not visible in trace (a). For weak feedback,  $\Delta i = 3.6\%$  [trace (b)], the second ECM (mode 2) is lasing; it is shifted by about 1 GHz to the longer wavelength. As  $\Delta i$  is increased to 4.4%, lasing is transferred to mode 3 [trace (d)]. The signal strength of traces (a)–(c) is too weak to infer the dynamical state of the system. Mode 3 is initially stable but with increasing  $\Delta i$  relaxation oscillation sidebands are undamped close to the frequency of the ECM spacing [13]. For a further increase in  $\Delta i$  we observe that the spectrum broadens, the center line decreases, and the sidebands become stronger [trace (e)]. This dynamical state is commonly referred to as coherence collapse and we typically observe dropout events. As we further increase  $\Delta i$  we find a regime of coexistences between the LFF regime and the next stable mode (mode 4). Mode 4 stabilizes for  $\Delta i = 5.6\%$  and the bifurcation series continues in this fashion. We observed this sequence for a total of 15 ECMs for the largest feedback strength accessible in our experiment.

Experimentally we have observed dropout events for  $\Delta i \approx 6.5\%$  in the fourth successive ECM. Figure 2(a) depicts a time trace for this regime clearly showing sharp drops in the laser intensity characteristic of bandwidth limited LFFs; Fig. 2(b) shows the corresponding optical spectrum indicating that the laser line has sidebands, and the corresponding power spectrum [Fig. 2(c)] clearly demonstrates the LFF peak which corresponds to the average time between dropout events [14]. Low-frequency fluctuations also occurred in the third ECM and may occur for even weaker feedback strength, but the signal strength is so weak that we cannot distinguish signal from noise.

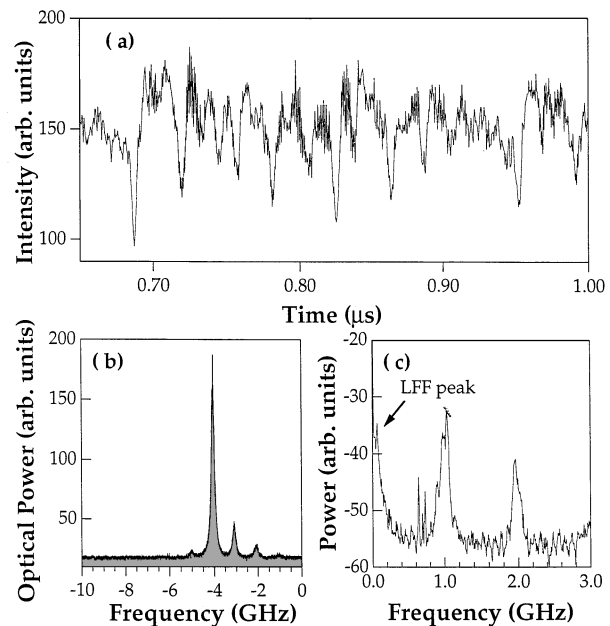


FIG. 2. Dropout events were observed for  $\Delta i \approx 6.5\%$ , when the fourth ECM becomes unstable. (a) The time trace clearly shows dropouts in the intensity. (b) The corresponding optical spectrum shows large sidebands on the lasing mode. (c) The power spectrum shows the characteristic LFF peak (arrow) and peaks at multiples of the inverse-round-trip time.

Throughout the bifurcation cascade we observed coexistences between the LFF regime and the next stable mode when the feedback strength was slightly weaker than required to stabilize the next higher mode. An example is shown in Fig. 3. For  $\Delta i \approx 9.5\%$  we observe both the unstable mode 5 and the stable mode 6. Figure 3(a) depicts a time trace showing regions of stable output and regions with large fluctuations. As we stretch the time scale in Fig. 3(b) we clearly observe dropout events and a stable region. Note that the time trace was captured with the ac-coupled detector; our calibrated dc-coupled detector measured intensities and standard deviations of  $0.46 \pm 0.04$  mW for the LFF state and  $0.05 \pm 0.01$  mW for the stable state. Figure 3(c) and 3(d) show the optical spectra of the stable state displaying a single mode with narrow linewidth and the LFF state which exhibits a broad line with many sidebands. Most times, however, we observed an optical spectrum composed of the characteristics of both spectra.

A single mode semiconductor laser subject to weak and moderate optical feedback is modeled with the Lang-Kobayashi equations [10]. The dimensionless rate equations for the complex electric field  $\mathcal{E}$  and the excess carrier number  $N$  are

$$\frac{d\mathcal{E}}{ds} = (1 + i\alpha)N\mathcal{E} + \kappa\mathcal{E}(s - \tau)\exp(-i\omega_0\tau), \quad (1)$$

$$T \frac{dN}{ds} = P - N - (1 + 2N)|\mathcal{E}|^2. \quad (2)$$

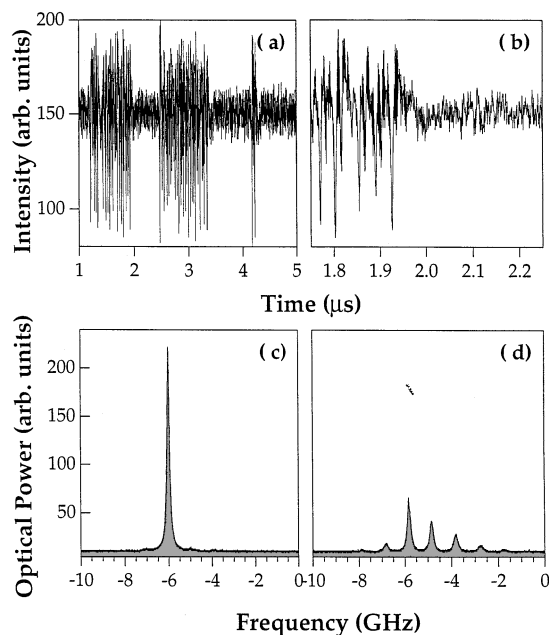


FIG. 3. Experimentally observed coexistences between LFFs and the stable maximum gain mode for  $\Delta i \approx 9.5\%$ . (a) The intensity exhibits regions of large fluctuations and of stable operation. (b) A magnification of the unstable regime demonstrating that the laser intensity exhibits dropout events. (c) A single narrow line for the stable regime and (d) many sidebands at the ECM spacing corresponding to the LFF regime.

In these equations time  $s$  is measured in units of the photon lifetime  $\tau_p$  ( $s \equiv t\tau_p^{-1}$ ). The external round-trip time is normalized as  $\tau \equiv 2L/c\tau_p$ .  $\omega_0 \equiv \omega\tau_p$  is the dimensionless angular frequency of the solitary laser  $\omega$  and  $\kappa \equiv \gamma\tau_p$  is the normalized feedback rate.  $\alpha$  is the linewidth enhancement factor and  $T$  is the ratio of the carrier  $\tau_s$  to photon lifetime  $\tau_p$  and the pumping rate above threshold  $P$ .

We numerically integrated Eqs. (1) and (2) with typical parameters for the semiconductor laser used in the experiment:  $\tau_p = 1.0$  ps,  $\tau_s = 1$  ns,  $T = 1000$ ,  $\tau = 1000$  ( $L = 15$  cm),  $\alpha = 4$ ,  $\omega_0\tau = -1$ , and  $P = 0.001$ . A bifurcation diagram is shown in Fig. 4. As the feedback strength  $\kappa$  is increased from zero the first ECM is initially stable and then undergoes a Hopf bifurcation, indicating the birth of sustained relaxation oscillations. The laser becomes unstable and chaotic via a period-doubling bifurcation. For  $\kappa = 0.0012$  the next higher ECM (mode 2) becomes stable and temporarily coexists with the unstable mode 1. For these values of  $\kappa$ , mode 2 is the maximum gain mode and is stable [11]. Mode 2 undergoes a Hopf bifurcation for  $\kappa = 0.0020$  and follows a quasiperiodic route into chaos which develops into LFFs for  $\kappa = 0.00305$  through a crisis. For a further increase in  $\kappa$  the next ECM (mode 3) is initially stable, then undergoes a Hopf bifurcation following a similar route into instabilities, and the bifurcation cascade continues.

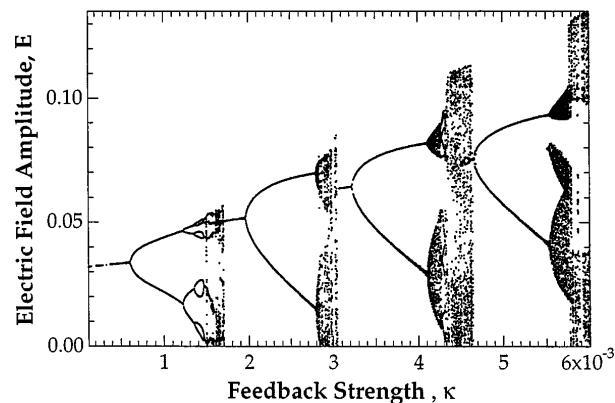


FIG. 4. Numerically computed bifurcation cascade for a single mode semiconductor laser pumped 0.001 above threshold and subject to weak optical feedback. As the feedback strength  $\kappa$  is increased from zero, the first ECM is stable and then becomes unstable through a Hopf bifurcation for  $\kappa = 0.0006$  and chaotic via a period-doubling bifurcation. For  $\kappa = 0.0012$  the next higher ECM (mode 2) becomes stable and coexists with the unstable mode 1. Mode 2 becomes unstable for  $\kappa = 0.0020$  and follows a quasiperiodic route into chaos. Stable mode 3 then becomes accessible to the system and coexists with the unstable attractor of mode 2, and then mode 3 also becomes unstable for  $\kappa = 0.0032$  and the bifurcation cascade continues.

The scenario for the onset of LFFs is as follows: The fixed points of the Lang-Kobayashi equations lie in an ellipse in the phase space spanned by the phase difference  $\phi(t) - \phi(t - \tau)$  and the carrier number  $N$ . As the feedback strength is increased, new fixed points are created in pairs by a saddle-node bifurcation. The fixed point associated with the initially stable node is denoted by filled circles, and the saddle, also called an antimode, is denoted by asterisks (Fig. 5). Two new fixed points are born for  $\kappa = 0.00273$ , mode 3, which are the maximum gain mode and the corresponding antimode. As  $\kappa$  is minutely increased the antimode moves closer to the unstable mode in phase space until it collides with the chaotic attractor for  $\kappa = 0.00305$ , causing a crisis. This destroys the chaotic attractor, and a chaotic saddle remains. The trajectory in Fig. 5 initially moves around the fixed point of mode 2, which was attracting (chaotic attractor) but is now destroyed and has become a chaotic saddle. The trajectory tries to reach the maximum gain mode but comes close to the antimode and is repelled; the intensity drops to zero. Again the trajectory climbs up to reach the maximum gain mode, stays for a while near the chaotic saddle of mode 2, comes close to the antimode, but this time is captured by the maximum gain mode and remains there.

We find stabilization regions throughout all of the LFF regime depicted in the bifurcation diagram in Fig. 4. For  $\kappa = 0.00762$ , for example, we find that the intensity initially pulsates but stabilizes after about 450 photon lifetimes. By plotting the trajectory in phase space we

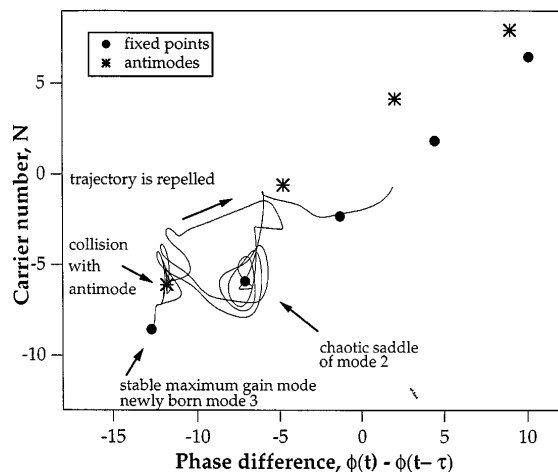


FIG. 5. Dropout events occur for as little feedback as  $\kappa = 0.00305$ . The system trajectory in phase space moves among five fixed points trying to reach the maximum gain mode. Yet, before it reaches the stable maximum gain mode, the trajectory collides with an unstable antimode (arrow), a crisis occurs, and the trajectory returns to zero intensity. Again the trajectory tries to reach the maximum gain mode; it moves around the chaotic saddle of mode 2, comes close to the antimode, but then is captured by the maximum gain mode and remains there.

verified that the trajectory has reached the maximum gain mode.

In summary, we have experimentally observed a series of successive bifurcations between stable and unstable ECMs in a single mode semiconductor laser system pumped near threshold and subject to optical feedback. The experimental observations are in very good agreement with the numerical computations based on the Lang-Kobayashi equations. We found that, contrary to previously held views, the maximum gain mode can be accessible to the system. We have observed coexistences between the stable maximum gain mode and LFFs experimentally. Numerically we observed that the trajectories

in the LFF regime stabilize at the maximum gain mode after sufficiently long integration. We have also observed experimentally that dropout events occur for very weak feedback, when only the third ECM is accessed; numerically we found LFFs in the second ECM. Thus unlike in [6] we find many stable regimes followed by instabilities for single mode lasers pumped near threshold. The observation of accessibility of the maximum gain mode is important for the possible stabilization of the system [15].

- 
- [1] M.C. Mackay and L. Glass, *Science* **197**, 287 (1977); J. Foss, A. Longtin, B. Mensour, and J. Milton, *Phys. Rev. Lett.* **76**, 708 (1996); K. Ikeda and K. Matsumoto, *Physica (Amsterdam)* **29D**, 223 (1987).
  - [2] D. Lenstra, B.H. Verbeek, and A.J. den Boef, *IEEE J. Quantum Electron.* **21**, 674 (1985); F. Mogenson, H. Oleson, and G. Jacobsen, *Electron. Lett.* **21**, 696 (1985); H.L. Wang, M.J. Freeman, and D.G. Steel, *Phys. Rev. Lett.* **71**, 3951 (1993).
  - [3] C. Risch and C. Voumard, *J. Appl. Phys.* **48**, 2083 (1977).
  - [4] I. Fischer *et al.*, *Phys. Rev. Lett.* **76**, 220 (1996).
  - [5] G.H.M. Tartwijk, A.M. Levine, and D. Lenstra, *IEEE J. Sel. Top. Quantum Electron.* **1**, 466 (1995).
  - [6] R.W. Tkach and A.R. Chraplyvy, *J. Lightwave Technol.* **4**, 1655 (1986).
  - [7] H. Temkin *et al.*, *J. Quantum Electron.* **22**, 286 (1986).
  - [8] P. Besnard, B. Meziane, K. Ait-Ameur, and G. Stephan, *IEEE J. Quantum Electron.* **30**, 1713 (1994).
  - [9] T. Sano, *Phys. Rev. A* **50**, 2719 (1994).
  - [10] R. Lang, and K. Kobayashi, *IEEE J. Quantum Electron.* **16**, 347 (1980).
  - [11] A.M. Levine *et al.*, *Phys. Rev. A* **52**, R3436 (1995).
  - [12] K.C. Harvey and C.J. Myatt, *Opt. Lett.* **16**, 910 (1991).
  - [13] G. Lythe *et al.*, *Phys. Rev. A* **55**, 4443 (1997).
  - [14] A. Hohl, Ph.D. thesis, Georgia Institute of Technology, 1995 (unpublished), Chap. 3.
  - [15] J. Wieland, C.R. Mirasso, and D. Lenstra, *Opt. Lett.* **22**, 469 (1997).